

## Neutron scattering from coupled phonon-impurity modes in $\text{KCl}_{1-c}(\text{KCN})_c$

R. M. Nicklow, W. P. Crummett,\* M. Mostoller, and R. F. Wood

*Solid State Division, Oak Ridge National Laboratory, Oak Ridge, Tennessee 37830*

(Received 14 April 1980)

The hybridization of host-lattice phonons with the internal-energy states of  $\text{CN}^-$  impurities in KCl has been studied by inelastic neutron scattering as a function of temperature between 10 and 100 K for samples with impurity concentrations in the range  $c = 0.4$  to 6 at. %. A temperature- and concentration-dependent coupling between phonons with  $E_g$  symmetry and the  $E_g$  transitions of  $\text{CN}^-$  ions is observed near a frequency of 0.5 THz, a value which is consistent with the energy-level spacings for  $\text{CN}^-$  in KCl as deduced by Beyeler. However, an expected coupling of phonons and  $\text{CN}^-$  transitions with  $T_{2g}$  symmetry near the same frequency was not detected. A simple two-level model for the  $\text{CN}^-$  impurity provides a rather good description of the data for the  $E_g$  coupled modes for  $c < 2$  at. %, but it deviates significantly for larger concentrations. Quasielastic scattering, which has a strong dependence on impurity concentration, temperature, and phonon wave vector, is also observed.

### INTRODUCTION

The influence of impurities on the phonon spectra of solids has been extensively studied both theoretically and experimentally. Neutron inelastic scattering has been one of the principal experimental techniques used in such studies owing to the very detailed information about phonon energies and lifetimes which can be obtained throughout the Brillouin zone. With very few exceptions almost all neutron scattering investigations to date have been carried out on systems in which the impurities were substitutional and monatomic. For low concentrations (<1 at. %) of such impurities, the influence on the phonon spectrum is generally small and difficult to measure because the perturbations to the dynamical equations of motion are relatively weak and vary smoothly with frequency.

This behavior is in sharp contrast to that which can occur when the defect possesses internal vibrational modes or internal energy states. In this case the perturbations introduced by the impurity are sharply peaked in frequency, with contributions to the dynamical matrix which are characterized by resonant-energy denominators of the form  $(\omega^2 - \omega_0^2)^{-1}$ , where  $\hbar\omega_0$  is an energy separating two of the internal states of the impurity. This leads to a resonant hybridization of the phonon modes with the impurity states, resulting in a coupled-mode spectrum which can be directly measured with neutrons even for concentrations as low as  $\sim 10^{-4}$ .

The first observation with neutrons of such a coupled-mode spectrum was carried out by Walton *et al.*<sup>1</sup> on KCl containing 0.37 at. %  $\text{CN}^-$  impurities. Substitutional  $\text{CN}^-$  impurities in the alkali halides exhibit a wide variety of motions including tunneling, libration, and free rotation.<sup>2</sup> Optical

experiments by Lüty<sup>3</sup> and by Beyeler<sup>4</sup> for  $\text{KCl}:\text{CN}^-$  indicate that the rotational ground state is a tunnel split multiplet involving the eight equivalent  $\langle 111 \rangle$  orientations of the  $\text{CN}^-$  ions. An approximate description of the energy levels for  $\text{CN}^-$  ions in KCl has been given by Beyeler,<sup>4,5</sup> who fitted a modified Devonshire potential to the observed level spacing in the ground-state multiplet and to the average splitting of the lowest excited states from the ground state. Ultrasonic measurements by Byer and Sack<sup>6</sup> indicate particularly strong coupling of the interlevel transitions to  $E_g$  and  $T_{2g}$  lattice modes. Results taken from Beyeler's papers are shown in Fig. 1, which also shows the allowed transitions involving  $E_g$  and  $T_{2g}$  phonons of the KCl host lattice.

Since the work reported in Ref. 1, we have un-

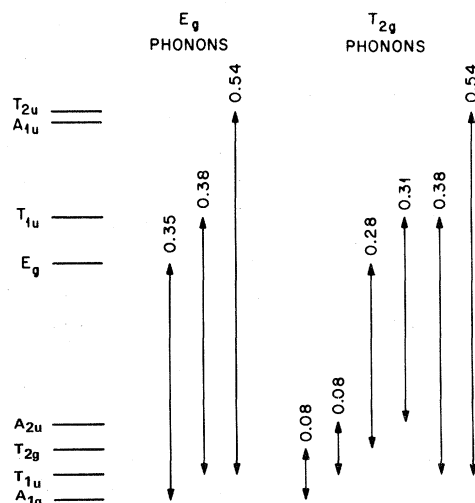


FIG. 1. Approximate energy-level spacings and allowed  $E_g$  and  $T_{2g}$  transitions (in units of terahertz) for  $\text{CN}^-$  in KCl, from Beyeler (Refs. 4 and 5).

dertaken a more comprehensive experimental and theoretical study of the KCl:CN<sup>-</sup> system. In spite of the complexity of the energy levels shown in Fig. 1, previous theoretical work<sup>7</sup> has indicated that a model containing only two levels provides a fairly good description of the wave-vector dependence of recent neutron scattering results for KCl (0.37 at. % CN<sup>-</sup>) at low temperature.<sup>8</sup> This model also yields predictions about the dependence of the coupled-mode spectrum on concentration and temperature, and in the present paper we present a comparison between theory and experimental results for these properties.

### THEORY

Although the theoretical treatment of the interaction between phonons and two-level defects in KCl has been presented previously,<sup>7</sup> we will briefly summarize the results here for completeness of the present report.

Along major symmetry directions in reciprocal space for cubic crystals, the coherent one-phonon cross section is branch diagonal:

$$S_{\text{coh}}(\tilde{q}j; \omega) \propto \text{Im} G(\tilde{q}j; \omega). \quad (1)$$

Here  $\tilde{q}$  is the scattering wave vector,  $j$  the branch index, and  $\hbar\omega$  is the energy transfer.  $G(\tilde{q}j; \omega)$  is the phonon Green's function, defined in the usual way<sup>9</sup> as the Fourier transform of the retarded displacement-displacement correlation functions. For a low concentration  $c$  of impurities, the Green's function is given by<sup>9</sup>

$$G(\tilde{q}j; \omega) = [\omega^2 - \omega^2(\tilde{q}j) - ct(\tilde{q}j; \omega)]^{-1}, \quad (2)$$

where  $\omega(\tilde{q}j)$  is a host-crystal phonon frequency, and  $t(\tilde{q}j; \omega)$  is the scattering matrix for a single impurity.

For an impurity with two energy levels at  $\pm\hbar\omega_0/2$  in the static lattice, the  $t$  matrix can be written in the form<sup>7, 10</sup>

$$t(\tilde{q}j; \omega) = \frac{\lambda^2 f_e (\omega_0 / \omega_r)}{\omega^2 - \Omega_0^2(\omega, T)} \langle \eta \rangle F(\tilde{q}j). \quad (3)$$

Here  $\lambda$  is a coupling parameter which scales as the square of a frequency,  $f_e$  is an oscillator strength, and  $F(\tilde{q}j)$  is a dimensionless geometrical factor.  $\Omega_0(\omega, T)$  is a complex, renormalized internal-mode frequency given by

$$\begin{aligned} \Omega_0^2(\omega, T) &= \text{Re}\Omega_0^2(\omega, T) + i\text{Im}\Omega_0^2(\omega, T) \\ &= \omega^2 - \lambda^2 f_e (\omega / \omega_r) g_T(\omega + i\epsilon). \end{aligned} \quad (4)$$

$\omega_r(T)$  is the frequency at which resonance occurs, determined self-consistently from Eq. (4) by  $\omega_r^2(T) = \text{Re}\Omega_0^2(\omega_r, T)$ . The imaginary and real parts of the temperature-dependent Green's function  $g_T$  in Eq. (4) are, respectively,

$$\begin{aligned} \text{Im}g_T(\omega) &= (\pi/2\omega) \coth(\hbar\omega/2kT) \\ &\times \sum_{\tilde{q}j} X^2(\tilde{q}j) \delta(\omega - \omega(\tilde{q}j)), \end{aligned} \quad (5)$$

$$\text{Re}g_T(\omega) = 2\pi\omega P \int_0^\infty d\omega' \frac{\text{Im}g_T(\omega')}{\omega'^2 - \omega^2}, \quad (6)$$

in which  $X^2(\tilde{q}j)$  gives the projection of the host-crystal mode specified by  $\tilde{q}j$  onto a suitably chosen local symmetrized coordinate  $X$ , involving the displacements of the neighbors of the impurity. Finally,  $\langle \eta \rangle \approx \tanh(\hbar\omega_r/2kT)$  represents the thermal-population difference between the ground and excited states of the impurity. Note that as this population difference decreases so does the strength of the phonon-impurity coupling.

The coherent neutron-scattering cross section is found by substituting the  $t$  matrix given by Eq. (3) into Eq. (2) for  $G(\tilde{q}j)$  and taking the imaginary part. The scattering cross section can exhibit either a two-peaked structure or a resonant-energy shift and line broadening, depending on the size of the damping represented by  $\text{Im}\Omega_0(\omega, T)$ .

We have used the two-level model corresponding to Eqs. (1)–(6) in extensive calculations, some of which are compared to the experimental results to be discussed later. In these calculations  $\text{Im}g_T(\omega)$  was determined by integrating over the Brillouin zone, and  $\text{Re}g_T(\omega)$  was then determined numerically from Eq. (6). Details of this type of calculation have been given elsewhere.<sup>11</sup> The symmetry coordinates  $X$  used for the calculation were the  $E_g$  modes of the six nearest neighbors of the CN<sup>-</sup> ion. The parameters  $\omega_0$  and  $\lambda^2 f_e$  were varied until a value of the resonance frequency, at the lowest temperature for which data were taken,  $\omega_r(T)$  was obtained that was in approximate agreement with the value of 0.54 THz shown in Fig. 1 for  $E_g$  phonons, and the splitting between the two peaks in the neutron scattering cross section was approximately that observed as discussed below (cf. Fig. 4). This procedure leads to parameters  $\nu_0 = \omega_0/2\pi = 1.75$  THz, and  $\lambda^2 f_e$  corresponding to a frequency  $\nu_1 = \sqrt{K/M}$ , where  $K = 18\,500$  dynes/cm and  $M$  is the mass of a potassium atom. These values suggest that the coupling between the impurity and the lattice is relatively strong.

### EXPERIMENTAL DETAILS

The crystals studied in the present work had nominal CN<sup>-</sup> concentrations of 0.37, 1.0, 2.4, and 5.9 at. %. A few measurements were also taken for pure KCl. The crystal with 0.37 at. % CN<sup>-</sup> is the same one studied previously by Walton *et al.*<sup>1</sup> It was grown by G. Schmidt of Cornell University and has approximate dimensions of  $2 \times 2 \times 5$  cm<sup>3</sup> with the [001] direction parallel to the longest

dimension. The other KCl:CN samples were obtained from F. Rosenberger of the University of Utah. They were grown from the melt and possessed a small variation ( $\sim 10\%$ ) in the concentration from the top to the bottom of the sample portion that was exposed to the neutron beam. These samples were approximately cylindrical in shape with diameters of about 2.5 cm and lengths between 2.5 and 5 cm, and with the [001] direction parallel to the cylindrical axis.

Judging from the clear optical appearance, the uniformity in the intensity across the neutron beam diffracted by each sample, and the angular sharpness of the Bragg peaks of each sample, we believe the CN<sup>-</sup> concentration was quite uniform throughout each sample (aside from the small variation from top to bottom mentioned earlier). The smooth concentration dependence of our results, as well as

those of Lüty<sup>12</sup> obtained on similar samples, seems to confirm this conclusion.

The experiments were performed on the triple-axis neutron spectrometers located at the HB-2 and HB-3 beam ports of the High Flux Isotope Reactor of the Oak Ridge National Laboratory. The (002) or (101) planes of Be crystals were used in various combinations as monochromator and analyzer. All measurements were carried out with the constant- $Q$  technique, with the scattered neutron energy fixed at 3.6 THz, and with a pyrolytic graphite filter located after the sample to suppress beam contamination. The beam collimation was generally  $10'$  and  $20'$  before and after the sample, respectively, giving a spectrometer resolution in the absence of focusing, of approximately 0.08 THz (full width at half maximum) for phonon frequencies in the range 0.0 to 1.0 THz. Some

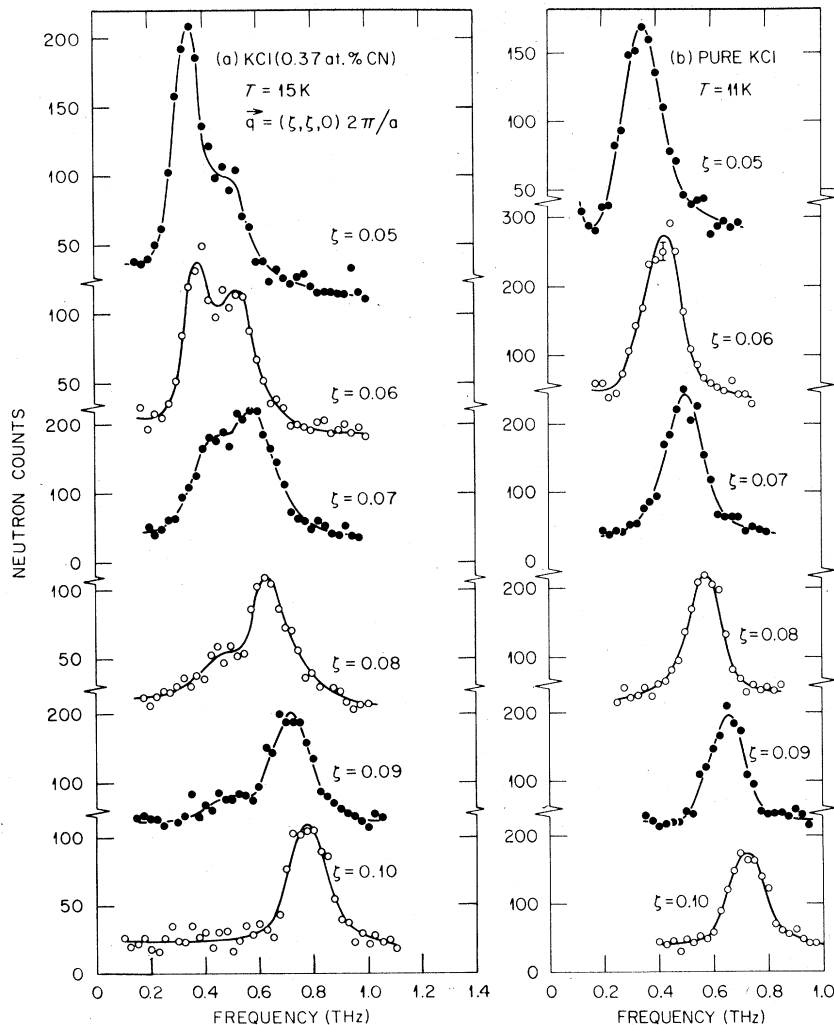


FIG. 2. The frequency distributions of neutrons scattered from (a) KCl (0.37 at. % CN<sup>-</sup>) and from (b) pure KCl at low temperature for the transverse-acoustic modes with  $\vec{q} = (\xi, \zeta, 0)2\pi/a$  and polarization in the  $[1\bar{1}0]$  direction.

measurements for the KCl-5.9 at. % CN<sup>-</sup> sample were obtained with collimations of 20' before and after the sample.

For each sample the transverse-acoustic-phonon branch with wave vectors  $\vec{q} = (\zeta, \zeta, 0)2\pi/a$  and with polarization in the  $[1\bar{1}0]$  direction ( $E_g$  symmetry) was studied for  $\zeta$  in the range 0.04 to 0.20 and for temperatures in the range 10 K to room temperature. As a shorthand notation, this branch hereafter will be designated as  $TA_1(\zeta\zeta 0)$ . Measurements were also carried out at 10 K on the transverse ( $T_{2g}$ )- and longitudinal ( $E_g$ )-acoustic branches in the  $[100]$  direction of the KCl-0.37 at. % CN<sup>-</sup> sample.

### RESULTS

The results obtained at 15 K for constant- $Q$  measurements of the  $TA_1(\zeta\zeta 0)$  branch are shown in Fig. 2(a) for  $\zeta = 0.05$  to 0.10 and for  $c = 0.37$  at. %. In Fig. 2(b) the corresponding scans obtained for pure KCl at 11 K are shown for comparison. There is a significant distortion or splitting of the phonon peaks in the crystal with impurities. The observed peak shapes are described very well by the sum of two Gaussian peaks as is illustrated by the lines drawn through the data in Fig. 2(a). The peak positions obtained from a fitting calculation based on the least-squares procedure are compared to the dispersion relation of pure KCl in Fig. 3. The dispersion curve for the crystal with defects shows a large splitting ( $\sim 0.15$  THz) near 0.5 THz, which represents the hybridization of these KCl phonons with one of the  $E_g$  transitions shown in Fig. 1. There appears to be no significant coupling of this phonon branch to the other  $E_g$  transitions near 0.35–0.38 THz shown in Fig. 1.

The data obtained for  $\zeta = 0.06, 0.07,$  and  $0.08$  are compared in Fig. 4 to a calculation based on the theory discussed above. The influence of the instrumental resolution has been taken into account approximately by folding the theoretical results at each wave vector with a Gaussian function of frequency with the appropriate experimental width. The theoretical results resemble the corresponding experimental curves, although the calculated peak splittings are too small and the wave-vector dependence of the calculated intensity variation is too strong. Nevertheless the agreement is quite good considering the simplicity of the model. Taking into account the wave-vector dependence of the instrumental resolution in the folding calculation may improve the agreement, but that does not seem to be warranted at present. Such a calculation would greatly increase the computational effort since theoretical curves would be required at many wave vectors.

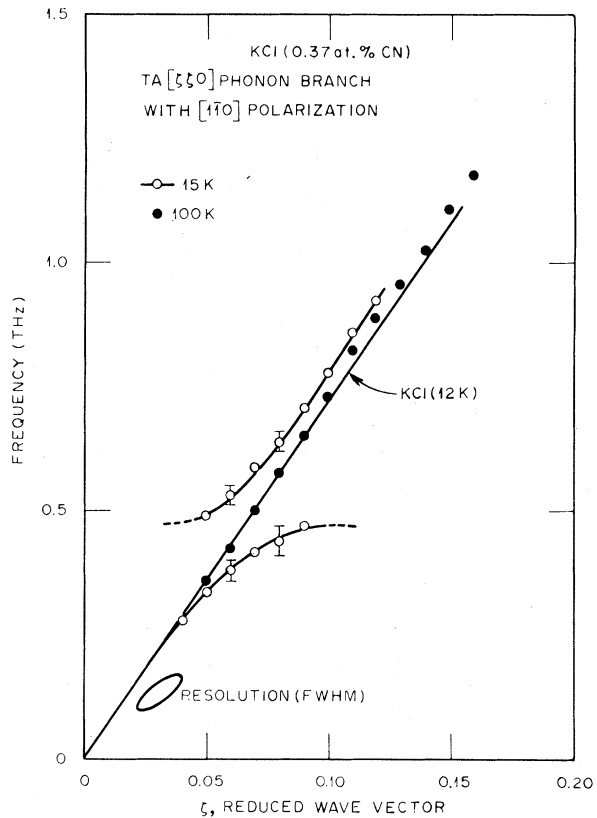


FIG. 3. The dispersion relation for the coupled-impurity  $TA_1(\zeta\zeta 0)$  phonon modes in KCl (0.37 at. % CN<sup>-</sup>) at 15 and 100 K compared to that for KCl.

The longitudinal-acoustic phonons with wave vectors in the  $[100]$  direction,  $LA(\zeta 00)$ , also possess  $E_g$  symmetry. Consequently they also couple to the  $E_g$  transitions of the CN<sup>-</sup> ions as is seen in Fig. 5 where measurements of these phonons for  $c = 0.37$  at. % and  $T = 15$  K are shown. Again we

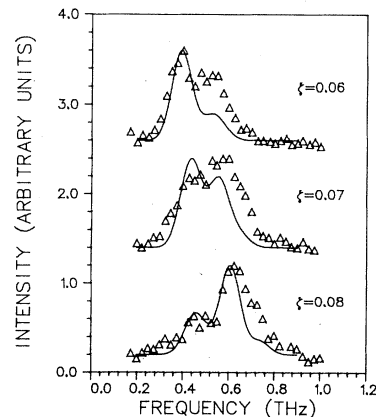


FIG. 4. Comparison of the experimental and theoretical line shapes for the coupled-impurity  $TA_1(\zeta\zeta 0)$  phonon modes in KCl (0.37 at. % CN<sup>-</sup>).

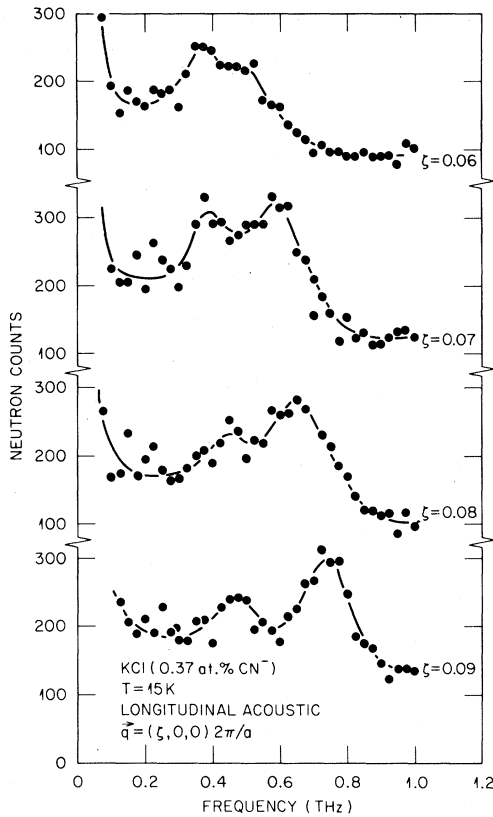


FIG. 5. The frequency distributions of neutrons scattered from the coupled-impurity LA( $\zeta 00$ ) phonon modes of KCl (0.37 at. %  $\text{CN}^-$ ) at 15 K.

have observed no significant coupling to the lower-energy  $E_g$  transitions near 0.3–0.4 THz.

The transverse-acoustic phonons in the [100] direction possess  $T_{2g}$  symmetry. However, these phonons do not couple significantly to any of the  $T_{2g}$  transitions of the  $\text{CN}^-$  ions which have frequencies accessible to our neutron measurements, i.e., above about 0.2 THz. Typical results for phonons with frequencies near 0.5 THz are shown in Fig. 6. No indication of peak splittings such as those seen in Fig. 2 for the  $\text{TA}_1(\zeta\zeta 0)$  branch is observed for the  $\text{TA}(\zeta 00)$  branch. However, the ultrasonic studies of Byer and Sack<sup>6</sup> show that the  $\text{TA}(\zeta 00)$  modes do couple to the very-low-frequency  $\text{CN}^-$  transitions with  $\nu \approx 0.1$  THz.

Our study of the concentration dependence of these phonon-defect interactions has been limited so far to the transverse  $\text{TA}_1(\zeta\zeta 0)$  phonon branch. Results for the concentration dependence of the intensity distribution at low temperature for a particular wave vector  $\zeta = 0.08$  are shown in Fig. 7. There are several noteworthy changes which occur with increasing  $\text{CN}^-$  concentration. The splitting of the two peaks increases, with the low-

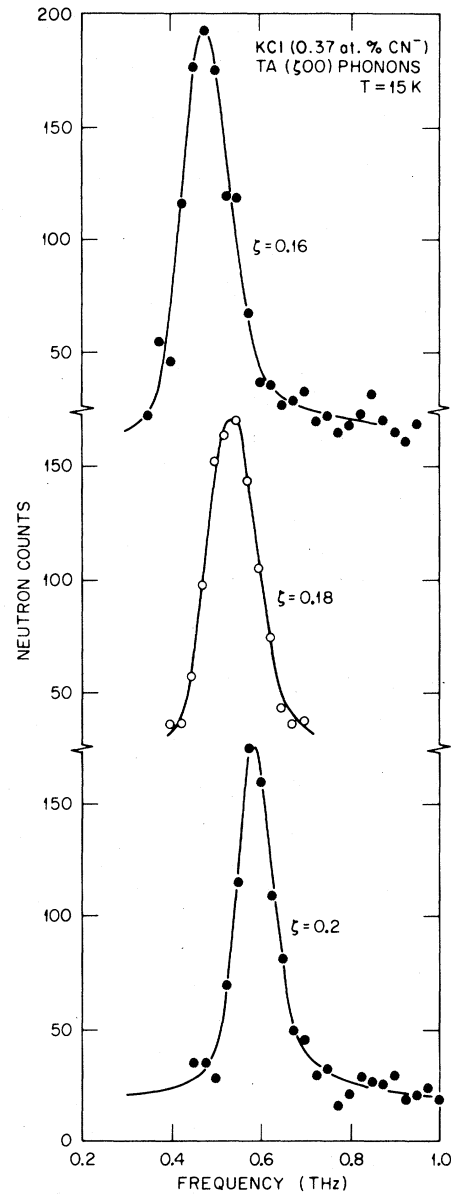


FIG. 6. The  $\text{TA}(\zeta 00)$  phonon peaks of KCl (0.37 at. %  $\text{CN}^-$ ) showing no visible coupling to the  $T_{2g}$  transitions of  $\text{CN}^-$  near 0.5 THz.

frequency peak seemingly gaining intensity relative to the high-frequency peak. Also the widths of such peaks increase, indicating an increase in damping. The width of the high-frequency peak at this wave vector changes quite strongly with  $\text{CN}^-$  concentration, becoming so large at  $c = 5.9$  at. % that only the low-frequency peak is observable. This damping behavior may be responsible for part of the observed changes in the relative intensities of the two peaks. However, this type of intensity variation is also predicted by the theory as shown in Fig. 8, even though it fails to reproduce the ob-

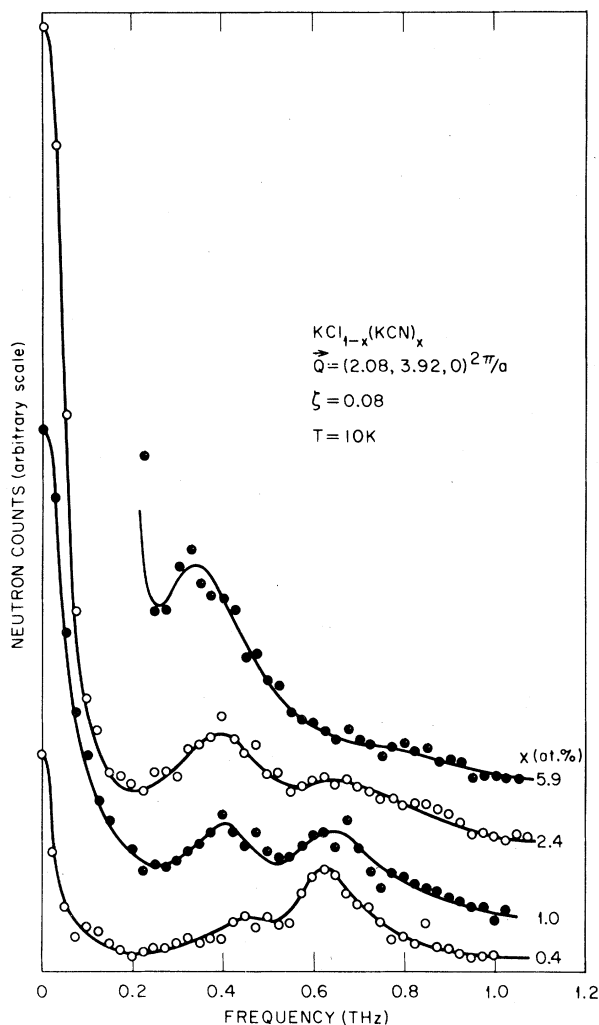


FIG. 7. The frequency distribution of scattered neutrons for the  $TA_1(\xi\xi 0)$  modes in  $KCl_{1-c}(KCN)_c$  for  $\xi = 0.08$ .

served width changes. It also fails to give sensible results for  $c \geq 3$  at.%. The failure of the model to reproduce the observed damping may indicate that the damping is related to the multilevel properties of the  $CN^-$  energy states, to defect-defect interactions, or to a nonuniform defect concentration in our samples. One final observation concerning the data displayed in Fig. 7 is the existence of a concentration-dependent intensity which peaks at  $\nu = 0$ . This scattering intensity also depends on both the wave vector  $\xi$  and the temperature as we shall discuss later.

The wave-vector dependence of the intensity distributions for  $c = 2.4$  at.% is shown in Fig. 9. These data are qualitatively similar to those for  $c = 0.37$  at.%. The most obvious difference, in addition to those discussed above, is that the peak splitting

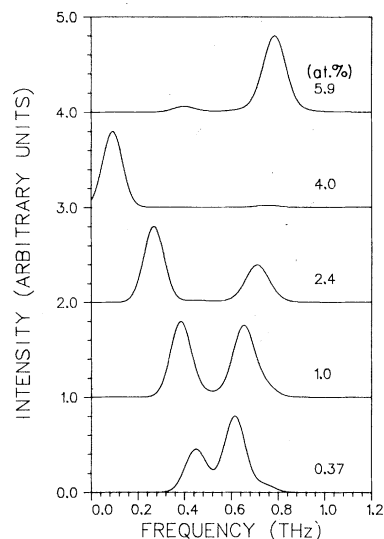


FIG. 8. Theoretical results for the concentration dependence of the neutron scattering by the coupled-impurity  $TA_1(\xi\xi 0)$  phonon modes for  $\xi = 0.08$  and  $T = 10$  K.

for  $c = 2.4$  at.% appears to occur at higher wave vectors. This result is consistent with the increase of the lower-frequency intensity with increasing  $CN^-$  concentration shown in Fig. 7. Apparently the wave vector corresponding to the resonance frequency varies from being just below  $\xi = 0.08$  for  $c = 0.37$  at.% to being just above for  $c = 2.4$  at.%.

We have attempted to deduce approximate dispersion curves from the data for each sample and these are compared in Fig. 10. Except for small  $c (\leq 1$  at.%), the concept of a dispersion curve may have little meaning. In view of the rather large energy widths of many of the observed peaks, it would probably be more appropriate to plot contours of constant intensity. However, in an effort to compare a portion of the results obtained for different defect concentrations in a single figure, we show in Fig. 10 the lines which roughly correspond to the loci of the intensity maxima for the two branches of the hybridized modes. This figure should be interpreted with caution, since for  $c > 1$  at.% the intensity distribution at each wave vector extends (see Fig. 7) from  $\nu = 0$  to a frequency well above that indicated by the line drawn. In any case one can see from Figs. 7–10 that the disturbance of the  $TA_1(\xi\xi 0)$  phonon branch increases substantially with increasing defect concentration.

The temperature dependence of the coupling between the  $TA_1(\xi\xi 0)$  phonons and the  $CN^-$ -impurity modes has also been studied in some detail. Portions of the results typical for  $c = 0.37$  at.% are shown in Figs. 3 and 11. As shown in Fig. 11 there is a strong temperature variation between 15 and

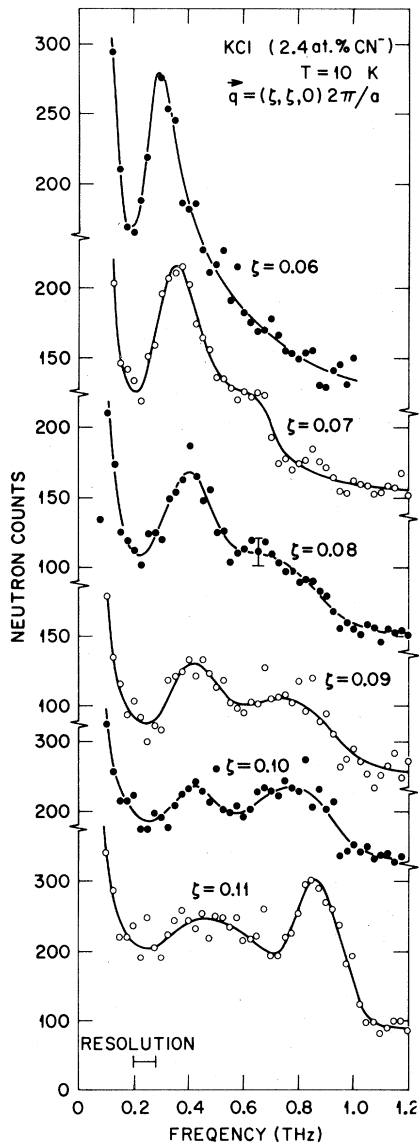


FIG. 9. The frequency distribution of neutrons scattered from the  $TA_1(\xi\xi 0)$  modes in KCl (2.4 at.%  $CN^-$ ) at 10 K.

40 K in the peak shapes for  $\zeta$  in the vicinity of the branch splitting. Within the experimental resolution, evidence for the peak splitting has essentially vanished by 40 K. This result is generally consistent with the theoretical calculations of the line shapes which are shown in Fig. 12. And, as is indicated in Fig. 3, at 100 K the dispersion curve for the mixed crystal is close to that for pure KCl. The small difference which remains is significant, however, and may indicate the existence of phonon coupling to other impurity levels at energies above those shown in Fig. 1. The temperature dependence observed for the phonon-

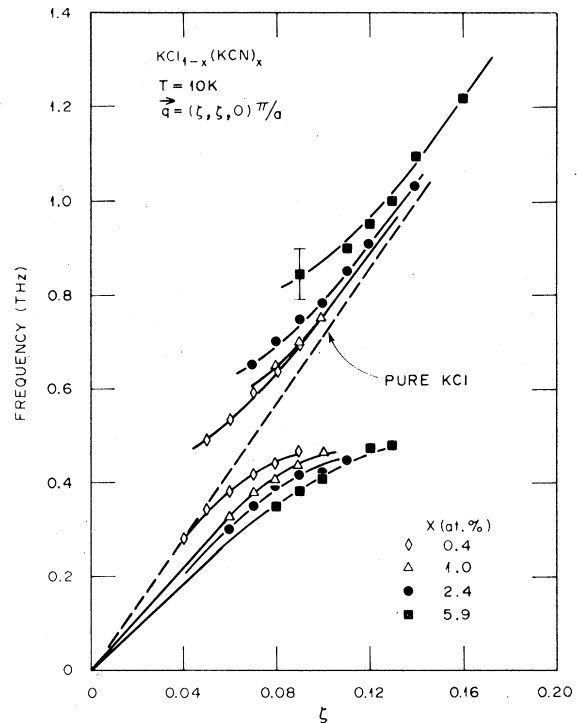


FIG. 10. The concentration dependence of the phonon-impurity mode hybridization for the  $TA_1(\xi\xi 0)$  phonons in  $KCl_{1-x}(KCN)_x$ .

defect coupling at the higher concentrations is qualitatively similar to that for  $c = 0.37$  at.%, with the exception that just above the temperature where the peak splittings vanish ( $\sim 40$  to  $50$  K), there remains a large distortion of the dispersion curve. This behavior is illustrated in Figs. 13 and 14 for  $c = 1.0$  at.%. The results shown in Fig. 14 for 40 K, for example, represent the wave-vector dependence of the peak maxima derived from data such as that shown in Fig. 13 for  $\zeta = 0.09$ . For this defect concentration (and up to 6%) the phonon-defect coupling as a function of temperature appears to vary from that expected for the small damping limit through that for the large damping limit before reaching the situation, at  $T \geq 100$ – $150$  K, corresponding to negligible coupling. This variation in the coupling behavior extends over an increasingly broader temperature range with increasing defect concentration. It is interesting that, as shown in Fig. 14, the predominant distortion of the dispersion curve at 40 K appears as only downward shifts (or softening) of the frequencies relative to those for pure KCl.

The origin of the scattering which peaks at  $\nu = 0$  has not yet been definitely established. The intensity of this scattering varies quite strongly with the  $CN^-$  concentration as is evident in the data

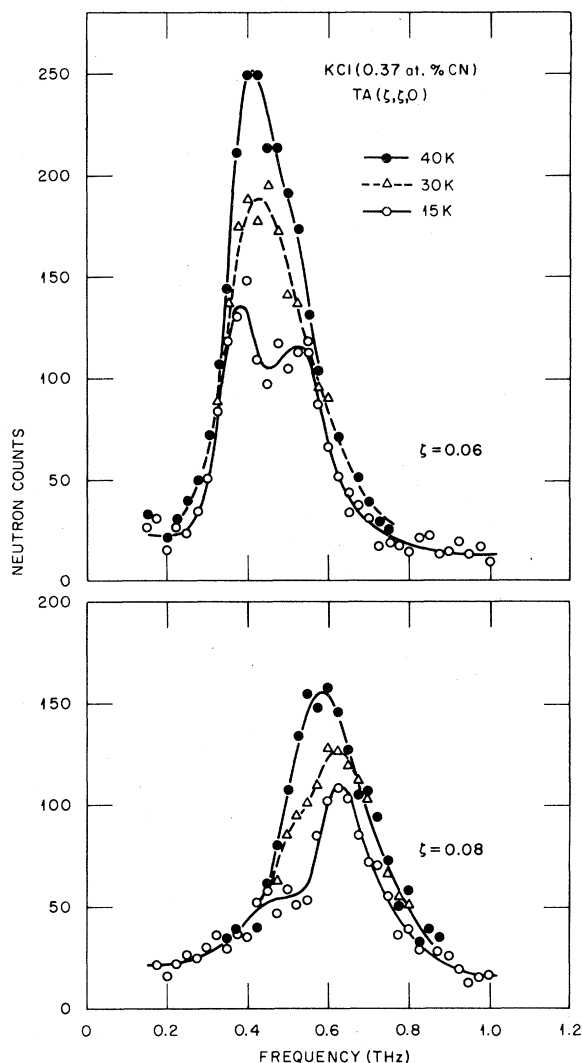


FIG. 11. The temperature dependence of the  $TA_1(\xi\xi 0)$  phonon-impurity mode coupling for KCl (0.37 at. %  $CN^-$ ).

shown in Fig. 7. It also varies with  $\vec{q}$  and  $T$  as shown in Fig. 15 for  $c = 2.4$  at. %. We have not yet studied in detail both the  $\vec{q}$  and  $T$  dependence of this scattering for each of our samples. The observed energy width is the same as that of the instrumental resolution, about 0.08 THz ( $\sim 0.3$  meV), at all of the  $c$ ,  $\vec{q}$ , and  $T$  (10–300 K) investigated so far. Also, the intensity is anisotropic with respect to the direction of  $\vec{q}$  about a reciprocal-lattice point. For example, the intensity at  $\vec{Q} = (4 + \xi, 0, 0)2\pi/a$  is approximately a factor of 2 larger than that at  $\vec{Q} = (4 - \xi, 0, 0)2\pi/a$ . These properties are suggestive of the Huang scattering which is often associated with the lattice strains resulting from point defects. The temperature dependence we have observed then suggests that as the rotational and librational motions of the  $CN^-$

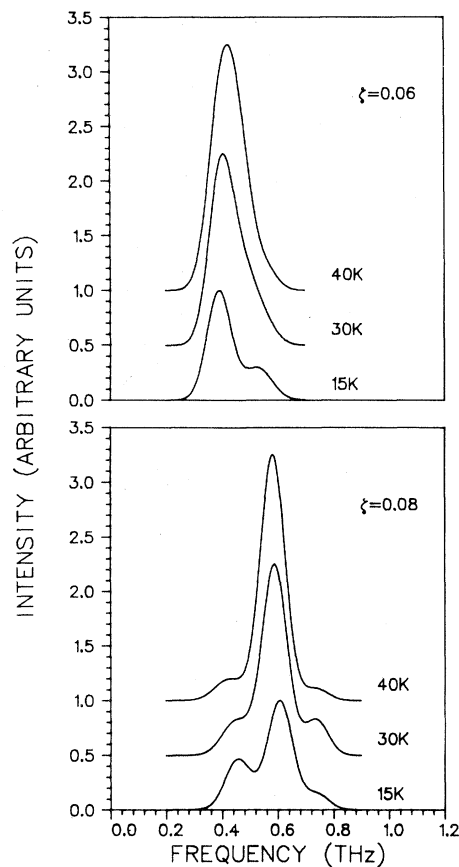


FIG. 12. Theoretical results for the temperature dependence of the phonon-impurity mode coupling in KCl (0.37 at. %  $CN^-$ ). The corresponding experimental results are shown in Fig. 11.

ions freeze out as the temperature is lowered, the magnitude of the lattice strain increases. Another interpretation may be possible in terms of the quasielastic scattering associated with the molecular orientational relaxation phenomena in mixed crystals as described by Michel *et al.*<sup>13</sup> However, the published calculations based on their theory all appear to show a significant energy width of such scattering, contrary to the present experimental results. Somewhat similar quasielastic scattering has also been observed recently in the more concentrated  $(KCN)_{0.5}(KBr)_{0.5}$  system by Rowe *et al.*<sup>14</sup> In that case the onset of the elastic scattering appears to be related to the softening of the  $TA(\xi 00)$  branch, and their interpretation involves the speculation of a phase change to a “dipole-glass” phase. Although we have observed no phonon softening, the concept of the  $CN^-$  orientations freezing in to produce a dipole glass may also apply to the dilute molecular impurity systems studied here. In any event this feature of the experimental results is quite interesting and warrants further investigation.



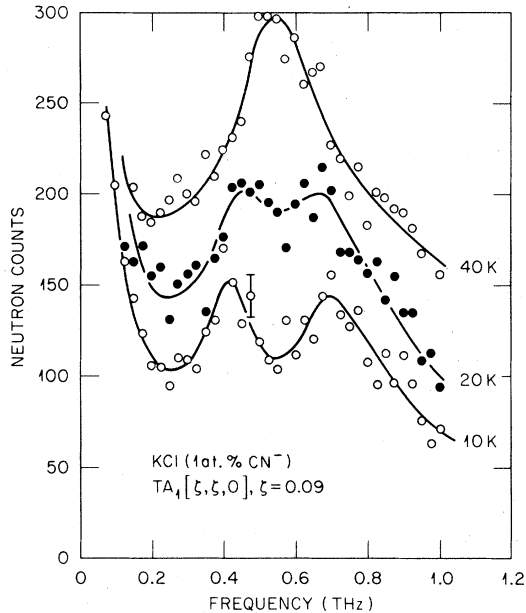


FIG. 13. The temperature dependence of the  $TA_1(\xi\xi 0)$ -impurity-mode scattering intensity for KCl (1 at. %  $CN^-$ ) and for  $\xi=0.09$ . The curves have been shifted vertically relative to each other for ease of comparison.

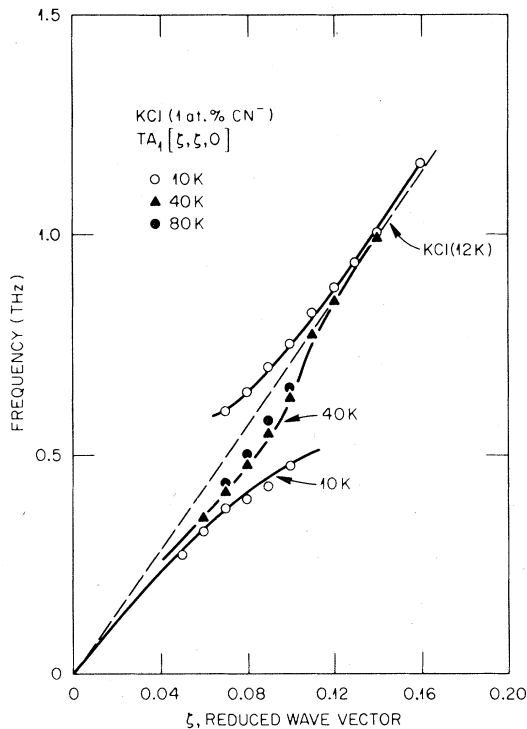


FIG. 14. The temperature dependence of the  $TA_1(\xi\xi 0)$  phonon-impurity mode coupling for KCl (1 at. %  $CN^-$ ).

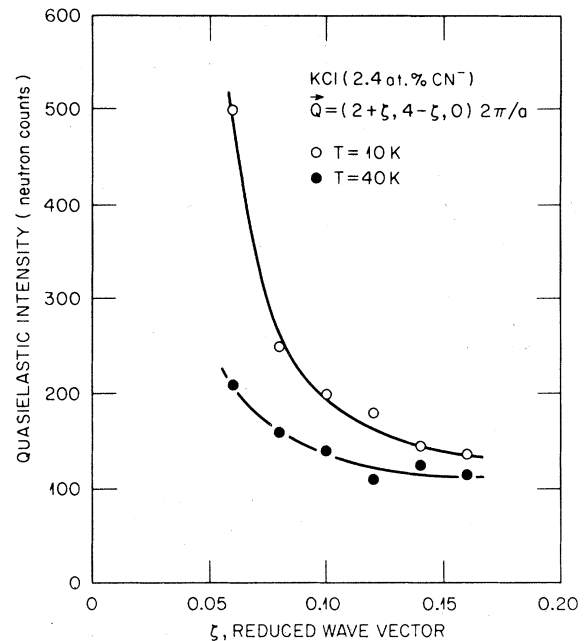


FIG. 15. Wave-vector and temperature dependence of the quasielastic scattering in KCl (2.4 at. %  $CN^-$ ).

#### SUMMARY

We have observed in neutron scattering experiments a coupling or hybridization of certain phonons in KCl with the internal-energy states of  $CN^-$  impurities. This coupling is very strong between phonons with  $E_g$  symmetry,  $TA_1(\xi\xi 0)$  and  $LA(\xi 00)$ , and the  $E_g$  transitions of  $CN^-$  near 0.5 THz. But it is unobservably small between  $TA(\xi 00)$  phonons and transitions having  $T_{2g}$  symmetry for frequencies in the range 0.2–1.0 THz.<sup>15</sup>

The simple two-level model for the  $CN^-$  impurities gives qualitatively good agreement with much of the neutron scattering data for different temperatures and concentrations for  $c \leq 2$  at.%. At larger concentrations the theory breaks down and it fails to explain the observed concentration dependence of the damping of the impurity-phonon coupled modes.

Quasielastic scattering is observed which varies with impurity concentration, temperature, and wave vector. The observed behavior of this scattering with temperature and wave vector suggests it is due to lattice strains which grow with decreasing temperature as the rotational and librational motions of the  $CN^-$  impurities freeze out.

*Note added.* The above results obtained at 10 K for  $c=0.37$  at.% are similar to the recent results of Rowe *et al.*<sup>16</sup> for  $CN^-$  in KBr. They also observe a coupling of the  $TA_1(\xi\xi 0)$  branch to an  $E_g$  transi-

tion of the  $CN^-$  ions near 0.4 THz but no coupling of the  $TA(\zeta 00)$  branch to a  $T_{2g}$  transition at such a high energy. However, they do observe a coupling of the  $TA(\zeta 00)$  branch to the  $T_{2g}$  tunneling transition at 0.07 THz between the levels of the tunnel-split ground state.

## ACKNOWLEDGMENT

This research was sponsored by the Division of Materials Sciences, U. S. Department of Energy under Contract No. W-7405-eng-26 with the Union Carbide Corporation.

\*Present address: Baptist College of Charleston, Charleston, South Carolina.

<sup>1</sup>D. Walton, H. A. Mook, and R. M. Nicklow, *Phys. Rev. Lett.* **33**, 412 (1974).

<sup>2</sup>V. Narayanamurti and R. O. Pohl, *Rev. Mod. Phys.* **42**, 201 (1970).

<sup>3</sup>F. Lüty, *Phys. Rev. B* **10**, 3677 (1974).

<sup>4</sup>H. U. Beyeler, *Phys. Rev. B* **11**, 3078 (1975).

<sup>5</sup>H. U. Beyeler, *Phys. Status Solidi* **52**, 419 (1972).

<sup>6</sup>N. E. Byer and H. E. Sack, *Phys. Status Solidi* **30**, 569 (1968).

<sup>7</sup>R. F. Wood and Mark Mostoller, *Phys. Rev. Lett.* **39**, 819 (1977).

<sup>8</sup>R. M. Nicklow, in *Proceedings of the Conference on Neutron Scattering*, edited by R. M. Moon (ORNL, Oak Ridge, Tennessee, 1976), Vol. 1.

<sup>9</sup>R. J. Elliott and D. W. Taylor, *Proc. R. Soc. London Ser. A* **296**, 161 (1967); Katya Lakatos and J. A. Krumhansl, *Phys. Rev.* **175**, 841 (1968).

<sup>10</sup>M. V. Klein, *Phys. Rev.* **186**, 839 (1969).

<sup>11</sup>R. F. Wood, in *Methods in Computational Physics* edited by B. Alder, S. Fernback, and M. Rothenberg (Academic, New York, 1976), Vol. 15.

<sup>12</sup>F. Lüty, *Ferroelectrics* **16**, 201 (1977).

<sup>13</sup>K. H. Michel, J. Naudts, and B. De Raedt, *Phys. Rev. B* **18**, 648 (1978).

<sup>14</sup>J. M. Rowe, J. J. Rush, D. J. Hinks, and S. Susman, *Phys. Rev. Lett.* **43**, 1158 (1979).

<sup>15</sup>A recent discussion of this problem has been given by R. C. Casella, *Phys. Rev. B* **20**, 5318 (1979).

<sup>16</sup>J. M. Rowe, J. J. Rush, S. M. Shapiro, D. G. Hinks, and S. Susman, *Phys. Rev. B* **21**, 4863 (1980).